https://doi.org/10.31489/2025M2/189-207 *Research article*

Exponentially fitted finite difference methods for a singularly perturbed nonlinear differential-difference equation with a small negative shift

T. Prathap, R. Nageshwar Rao*

School of Advanced Sciences, Vellore Institute of Technology, Vellore, India
(E-mail: prathapkumar07@gmail.com, nag.ragi@gmail.com)

This study presents exponentially fitted finite difference methods for solving a singularly perturbed nonlinear differential-difference equation that consists of a small negative shift. The quasilinearization technique is applied to the nonlinear problem and a sequence of linear problems is obtained. The resulting linear problems are treated with exponentially fitted finite difference methods of higher order. The methods developed in this paper are studied for stability and convergence. Numerical results using the proposed methods are presented for two test problems and hence the efficiency of the methods is demonstrated.

Keywords: singular perturbation theory, nonlinear, delay differential equations, differential-difference equations, boundary value problems, finite difference scheme.

2020 Mathematics Subject Classification: 65L10, 65L11.

Introduction

Singularly perturbed nonlinear differential equations pose significant challenges in various fields of engineering and applied science [1]. As a result of the nonlinearity, the perturbation parameter, and the delay parameter, these problems become more challenging to solve. Lange and Miura [2] initiated the analysis of singularly perturbed nonlinear differential-difference equations and explored the existence and uniqueness of solutions to these boundary value problems.

A B-spline collocation method was proposed by Kadalbajoo and Kumar in [3] to solve a singularly perturbed nonlinear differential-difference equation with a negative shift. In an effort to improve the accuracy of the exact solution in the boundary layer region, they developed a piecewise uniform mesh. Ravi Kanth and Murali [4] developed an exponentially fitted spline method to solve nonlinear singularly perturbed delay differential equations. The same authors in [5] presented a numerical technique for solving a certain type of nonlinear singularly perturbed delay differential equation, which utilizes parametric cubic splines and a special mesh structure.

Lalu and Phaneendra [6] proposed a computational method for nonlinear delay differential equations, which consists of the reduction of the nonlinear problem into a sequence of linear problems using the quasilinearization technique and trigonometric spline approach suggested to solve the sequence of singularly perturbed linear delay differential equations. Chandru et al. [7] utilized a hybrid difference scheme on a Shishkin mesh to solve a singularly perturbed reaction-diffusion problem with a discontinuous source term.

The authors Sirisha et al, in [8] introduced a mixed finite difference approach for solving singularly perturbed differential-difference equations with mixed shifts by applying domain decomposition. Subburayan and Ramanujam [9] provided uniformly convergent finite difference methods with piecewise

*Corresponding author. *E-mail: nag.ragi@gmail.com*

This research was funded by the National Board for Higher Mathematics, Department of Atomic Energy, Government of India, through project No. 02011/8/2021 NBHM(R.P)/R&D II/7224, dated 24.06.2021.

Received: 4 July 2024; *Accepted:* 18 March 2025.

linear interpolation on Shishkin meshes to solve singularly perturbed boundary value problems for second order ordinary delay differential equations of convection-diffusion type.

Woldaregay and Duressa [10] proposed the numerical treatment of singularly perturbed differential difference equations involving mixed small shifts in the reaction terms. Woldaregay and Duressa [11] devised a fitted operator mid-point upwind finite difference technique for solving a singularly perturbed differential equation with a small delay in convection and reaction terms. Ranjan and Gowrisankar [12] developed numerical methods for linear convection-diffusion singular perturbation problems on Shishkin mesh utilizing the non-symmetric discontinuous Galerkin finite element method with interior penalty methods.

Prathap and Rao [13] presented a uniformly convergent finite difference technique on a uniform mesh, for solving singularly perturbed boundary value problems of second order ordinary differential-difference equation of convection-diffusion type. The same authors in [14], developed numerical techniques using non-polynomial splines for singularly perturbed boundary value problems with mixed shifts on a Shishkin mesh. Chakravarthy and Kumar [15] developed a numerical technique utilizing an adaptive grid to solve a time-dependent singularly perturbed differential-difference convection-diffusion problem.

Kumar [16] proposed the numerical solution using the Shishkin mesh for a class of time-dependent singularly perturbed convection-diffusion problems containing retarded terms. Ranjan and Prasad [17] employed an exponentially fitted three-term finite difference method to approximate the solution of a singularly perturbed differential equation with small shifts. Rao and Chakravarthy [18] presented exponentially fitted finite difference methods for a class of time-dependent singularly perturbed one-dimensional convection diffusion problems with small shifts.

Kiltu et al. [19] presented a method for solving singularly perturbed delay reaction-diffusion equations with layers or oscillatory behavior. Tefera et al. [20] introduced a new fitted operator method for a singularly perturbed parabolic convection-diffusion problem. Vivek and Rao [21] presented one-dimensional singularly perturbed parabolic partial differential difference equations with mixed shifts using fitted operator spline in compression and adaptive spline methods. Chakravarthy et al. [22] presented the numerical solution using spline in tension on a uniform mesh for second-order singularly perturbed delay differential equations. Hassen and Duressa [23] developed a non-classical numerical method to solve a class of singularly perturbed delay parabolic convection-diffusion problems with Dirichlet boundary conditions.

It is widely recognized that classical numerical approaches yield erroneous results when applied to problems with smaller values of the perturbation parameter. Also, the nonlinearity in the equation poses challenges during discretization. Hence effective numerical techniques are needed to solve these equations, whose precision remains constant regardless of the perturbation parameter and also converges consistently. This motivates us to develop parameter-uniformly convergent numerical methods for singularly perturbed nonlinear boundary value problems with negative shift. In the present study we use the methods described in [24] and [25] for solving nonlinear boundary value problems and develop fitted operator finite difference methods for the linearized problem.

The following is the content arrangement in this paper. In Section 1, we provide a description of the problem being investigated and outline the necessary smoothness requirements for functions. Also, the quasilinearization technique is discussed, by which, the nonlinear differential equation is linearized and a sequence of linear equations is obtained and the convergence of the sequence of equations is studied. In Section 2, a modified form of the sequence of linear equations is obtained and some basic properties of the analytical solution are discussed. The numerical schemes for these linear problems are described in Section 3 and also the convergence analysis of the methods is carried out. Section 4 presents the numerical results for the test problems, while Section 5 provides the discussion and conclusions.

1 Statement of the problem

The following nonlinear differential-difference equation with a singular perturbation is considered:

$$\epsilon y'' = f\left(x, y(x), y'(x-\delta)\right), \ 0 \le x \le 1 \tag{1}$$

subject to the interval and the boundary conditions

$$y(x) = \phi(x); \ -\delta \le x \le 0, \text{ and } y(1) = \beta, \tag{2}$$

where $0 < \epsilon \ll 1$ is a singular perturbation parameter and δ is the shift parameter such that $0 < \delta < \epsilon$. The function $y(x)$ in (1)–(2) is assumed to be continuous across the interval $[0, 1]$ and has continuous derivatives over the open interval $(0, 1)$.

It is also assumed that $f\left(x, y(x), y'(x-\delta)\right) = \hat{f}(x, y, z)$, which is a smooth function that satisfies the following conditions:

- $\frac{\partial \hat{f}}{\partial y} > 0, \quad \frac{\partial \hat{f}}{\partial z} \le 0, \quad \frac{\partial \hat{f}}{\partial y} - \frac{\partial \hat{f}}{\partial z} \ge M > 0$, where M is a constant with a positive value.
- The growth constraint $\hat{f}(x, y, z) = O(z^2)$ as $z \to \infty$ for all real y and z and all $x \in [0, 1]$.

The problem (1)–(2) has a unique solution when $\delta = 0$ and the conditions stated above are satisfied.

1.1 The Quasilinearization Technique

We apply the quasilinearization process [26] described below to develop a numerical scheme for the nonlinear problem (1)–(2):

- An initial guess $y^{(0)}(x)$ for the solution of the problem (1) is considered, which also satisfies the interval and boundary conditions

$$y^{(0)}(x) = \phi(x), \ -\delta \le x \le 0, \ y^{(0)}(1) = \beta.$$

- Then the following sequence of boundary value problems is obtained:

$$\epsilon y''^{(k+1)}(x) = f\left(x, y^{(k)}(x), y'^{(k)}(x-\delta)\right), \tag{3}$$

  with $y^{(k+1)}(x) = \phi(x), \ -\delta \le x \le 0, \ y^{(k+1)}(1) = \beta$.
- After expanding the right-hand side of equation (3) in terms of Taylor series around $y^{(k)}$, we get

$$\begin{aligned} \epsilon y''^{(k+1)}(x) =& f\left(x, y^{(k)}(x), y'^{(k)}(x-\delta)\right) + \left(y'^{(k+1)}(x-\delta) - y'^{(k)}(x-\delta)\right)\left(\frac{\partial f}{\partial y'}\right)^{(k)} \\ &+ \left(y^{(k+1)}(x) - y^{(k)}(x)\right)\left(\frac{\partial f}{\partial y}\right)^{(k)} + \dots \end{aligned} \tag{4}$$

- We get the recurrence relation for the singularly perturbed linear differential-difference equations by modifying the terms of (4).

$$\begin{aligned} &\epsilon y''^{(k+1)}(x) - \left(\frac{\partial f}{\partial y'}\right)^{(k)} y'^{(k+1)}(x-\delta) - \left(\frac{\partial f}{\partial y}\right)^{(k)} y^{(k+1)}(x) = f^{(k)}\left(x, y^{(k)}(x), y'^{(k)}(x-\delta)\right) \\ &- \left(\frac{\partial f}{\partial y}\right)^{(k)} y^{(k)}(x) - \left(\frac{\partial f}{\partial y'}\right)^{(k)} y'^{(k)}(x-\delta), \text{ with } y^{(k+1)}(x) = \phi(x), \ -\delta \le x \le 0, \ y^{(k+1)}(1) = \beta. \end{aligned} \tag{5}$$

- For simplicity, we denote

$$a^{(k)}(\chi) = -\left(\frac{\partial f}{\partial y'}\right)^{(k)}, \quad b^{(k)}(\chi) = -\left(\frac{\partial f}{\partial y}\right)^{(k)}$$

and

$$r^{(k)}(\chi) = f^{(k)}\left(\chi, y^{(k)}(\chi), y'^{(k)}(\chi-\delta)\right) - \left(\frac{\partial f}{\partial y}\right)^{k} y^{(k)}(\chi) - \left(\frac{\partial f}{\partial y'}\right)^{(k)} y'^{(k)}(\chi-\delta)$$

so that (5) can be written as

$$\epsilon y''^{(k+1)}(\chi) + a^{(k)}(\chi) y'^{(k+1)}(\chi-\delta) + b^{(k)}(\chi) y^{(k+1)}(\chi) = r^{(k)}(\chi), \tag{6}$$

with the interval and boundary conditions

$$y^{(k+1)}(\chi) = \phi(\chi), \ -\delta \le \chi \le 0, \quad y^{(k+1)}(1) = \beta. \tag{7}$$

Therefore, for $k = 0, 1, 2, \ldots$, we solve the sequence of linear equations (6) subject to the interval and boundary conditions (7) rather than the original nonlinear problem (1)–(2). The solutions $y^{(k)}(\chi)$ converge to the solution $y(\chi)$ of the original nonlinear differential equation for large values of k. However, numerically, we require that $|y^{(k+1)}(\chi) - y^{(k)}(\chi)| < \mu, \ 0 \le \chi \le 1$, where μ is the imposed tolerance. The iterations can be terminated if the aforementioned requirements are satisfied, resulting in the solution to equations (1)–(2).

The convergence of the sequence of solutions of (6)–(7) is given in the form of the Lemma below:

Lemma 1. If $\langle \psi^{(k)} \rangle$ is the sequence of solutions of (6)–(7), $k = 0, 1, 2, \ldots$, then

$$\max_{0\le x\le 1} \left| \left(\psi^{(k+1)} - \psi^{(k)}\right)(\chi) \right| \le \kappa_1 \max_{0\le\chi\le 1} \left(\psi^{(k)} - \psi^{(k-1)}\right)^2, \ \kappa_1 < 1.$$

Proof. Consider the sequence of solutions $\langle \psi^{(k)} \rangle, \ k = 0, 1, 2, \ldots$ obtained by quasilinearization of (1)–(2).

With $\psi^{(0)}(\chi)$ as the initial approximation, equation(3) yields:

$$\epsilon \psi''^{(k)}(\chi) = f^{(k-1)} + \left(\psi^{(k)} - \psi^{(k-1)}\right) f_\psi(\psi^{(k-1)}), \tag{8}$$

where $f^{(k)} = f\left(x, \psi^{(k)}(\chi), \psi'^{(k)}(\chi-\delta)\right)$ and $f_\psi = \frac{\partial f}{\partial \psi}$.

From equation (3) and equation (8), we have

$$\epsilon \left(\psi^{(k+1)} - \psi^{(k)}\right)''(\chi) = f^{(k)} - f^{(k-1)} - \left(\psi^{(k)} - \psi^{(k-1)}\right) f_\psi(\psi^{(k-1)}) + \left(\psi^{(k+1)} - \psi^{(k)}\right) f_\psi(\psi^{(k)}). \tag{9}$$

Equation (9) is a second order dfferential equation in $\left(\psi^{(k+1)} - \psi^{(k)}\right)$. By using Green's function, equation (9) will be equivalent to the following integral form

$$\begin{aligned} \epsilon \left(\psi^{(k+1)} - \psi^{(k)}\right)(\chi) = \int_0^1 \mathcal{G}(\chi, s) \Big[& f^{(k)} - f^{(k-1)} - \left(\psi^{(k)} - \psi^{(k-1)}\right) f_\psi(\psi^{(k-1)}) \\ & + \left(\psi^{(k+1)} - \psi^{(k)}\right) f_\psi(\psi^{(k)}) \Big] ds. \end{aligned} \tag{10}$$

The Green's function $\mathcal{G}(\chi, s)$ is determined by

$$\mathcal{G}(\chi, s) = \begin{cases} (\chi - 1)s, \ 0 \le s \le \chi \le 1, \\ \chi(s-1), \ 0 \le \chi \le s \le 1, \end{cases}$$

where $\max\limits_{\chi,s} |\mathcal{G}(\chi, s)| = 1/4$.

Applying the mean value theorem [4], we can conclude that

$$f^{(k)} - f^{(k-1)} = \left(\psi^{(k)} - \psi^{(k-1)}\right) f_\psi(\psi^{(k-1)}) + \frac{\left(\psi^{(k)} - \psi^{(k-1)}\right)^2}{2} f_{\psi\psi}(\theta), \tag{11}$$

where $\psi^{(k-1)} \le \theta \le \psi^{(k)}$.

By replacing the expression (10) with equation (11), we obtain

$$\epsilon\left(\psi^{(k+1)} - \psi^{(k)}\right) = \int_0^1 \mathcal{G}(\chi, s)\left[\left(\psi^{(k)} - \psi^{(k-1)}\right)^2 f_{\psi\psi}(\theta)/2 + \left(\psi^{(k+1)} - \psi^{(k)}\right) f_\psi(\psi^{(k)})\right] ds. \tag{12}$$

Let $\max_{\|\psi\|\le 1} f_\psi(\psi) = a_1, \ \max_{\|\psi\|\le 1} f_{\psi\psi}(\psi) = a_2$. By evaluating the largest absolute value over the entire domain of interest for both sides of equation (12), we obtain

$$\begin{aligned} \max_{0\le\chi\le 1} \left| \left(\psi^{(k+1)} - \psi^{(k)}\right)(\chi)\right| \le & \frac{1}{4\epsilon}\int_0^1 \left[\max_{0\le\chi\le 1} \frac{\left(\psi^{(k)} - \psi^{(k-1)}\right)^2}{2} \max_{0\le\chi\le 1} |f_{\psi\psi}(\theta)| \right. \\ & \left. + \max_{0\le\chi\le 1} \left| \left(\psi^{(k+1)} - \psi^{(k)}\right)\right| \max_{0\le\chi\le 1} |f_\psi(\psi^{(k)})|\right] ds. \end{aligned}$$

Through the process of simplification, we obtain the following result:

$$\max_{0\le\chi\le 1} \left|\left(\psi^{(k+1)} - \psi^{(k)}\right)(\chi)\right| \le \kappa_1 \max_{0\le\chi\le 1} \left(\psi^{(k)} - \psi^{(k-1)}\right)^2,$$

since $\kappa_1 = a_2/(8\epsilon(1 - a_1/4\epsilon)) < 1$.

This demonstrates that the series $\langle\psi^{(k)}\rangle$ of linear equations converges quadratically if $\kappa_1 < 1$, thus satisfying the lemma.

2 *Continuous problem*

Assuming that the delay parameter δ is smaller than the perturbation parameter ϵ, the expression $y'^{(k+1)}(\chi - \delta)$ can be expanded using Taylor's series and hence the sequence of problems (6)–(7) is transformed into a sequence of boundary value problems:

$$(\epsilon - \delta a^{(k)}(\chi))y''^{(k+1)}(\chi) + a^{(k)}(\chi)y'^{(k+1)}(\chi) + b^{(k)}(\chi)y^{(k+1)}(\chi) = r^{(k)}(\chi), \tag{13}$$

subject to

$$y^{(k+1)}(0) = \phi(0), \ y^{(k+1)}(1) = \beta. \tag{14}$$

For $\delta = 0$, the solution of the above problem shows a boundary layer on either the left or right side of the interval, depending on the sign of the coefficient $a^{(k)}(\chi)$. Specifically, if $a^{(k)}(\chi) > 0$, the boundary layer is on the left side, and if $a^{(k)}(\chi) < 0$, the boundary layer is on the right side. Here, we consider $\delta \ne 0$ but comparable to ϵ, to study the effects on the boundary layer behavior of the solution to the problem (1). We presuppose that $a^{(k)}(\chi) \ge \mathscr{M} > 0$ and $b^{(k)}(\chi) \le -\theta < 0$ for positive constants $\mathscr{M}, \theta$.

We define the operator

$$\mathscr{L}(\pi(\chi)) \equiv \mu^{(k)}(\chi))\pi''^{(k+1)}(\chi) + a^{(k)}(\chi)\pi'^{(k+1)}(\chi) + b^{(k)}(\chi)\pi^{(k+1)}(\chi) = r^{(k)}(\chi),$$

where $\mu^{(k)}(\chi)) = (\epsilon - \delta a^{(k)}(\chi))$, and hence from the following Lemma, show that $\mathscr{L}(\pi(\chi))$ satisfies the minimum principle:

Lemma 2. If $\pi(s)$ is a smooth function satisfying the conditions $\pi(0) \geq 0$ and $\pi(1) \geq 0$, then $\mathscr{L}\left(\pi^{(k+1)}(s)\right) \geq 0$ for s in the interval $[0,1]$, whenever $\pi^{(k+1)}(s) \leq 0$ for s in the interval $(0,1)$.

Proof. Let us consider $z \in [0,1]$ be such that $\pi^{(k+1)}(z) = \min_{s\in[0,1]} \pi^{(k+1)}(s)$ and suppose that $\pi^{(k+1)}(z) < 0$. It is evident that $z \notin \{0,1\}$. Consequently, $\pi'^{(k+1)}(z) = 0$ and $\pi''^{(k+1)}(z) \geq 0$.

So we have, $\mathscr{L}\pi^{(k+1)}(z) = \mu^{(k)}(z)\pi''^{(k+1)}(z) + a^{(k)}(z)\pi'^{(k+1)}(z) + b^{(k)}(z)\pi^{(k+1)}(z) > 0$. This contradicts our assumption that $\pi^{(k+1)}(z) < 0$.

Thus, it follows that $\pi^{(k+1)}(z) \geq 0$ so $\pi^{(k+1)}(s) \geq 0$ for every s in the interval $[0,1]$.

The following lemma provides the stability estimate for the solution of the continuous problem (13).

Lemma 3. Let $y^{(k+1)}(\chi)$ denote the solution to equations (13) and (14), then $\|y^{(k+1)}\| \leq \theta^{-1}\|r^{(k)}\| + \max(|\phi_0|, |\beta|)$, here $\|.\|$ is $\mathscr{L}_\infty$ norm given by $\|y^{(k+1)}\| = \max_{s\in[0,1]} |y^{(k+1)}(s)|$.

Proof. We define two barrier functions $\psi^{\pm}$ as follows:

$$\psi^{\pm}(\chi) = \Theta^{-1}\|r^{(k)}\| + \max(|\phi_0|, |\beta|) \pm y^{(k+1)}(\chi).$$

Then we have $\psi^{\pm}(0) = \Theta^{-1}\|r^{(k)}\| + \max(|\phi_0|, |\beta|) \pm y^{(k+1)}(0),$ since $y^{(k+1)}(0) = \phi_0 \geq 0$. Furthermore $\psi^{\pm}(1) = \Theta^{-1}\|r^{(k)}\| + \max(|\phi_0|, |\beta|) \pm y^{(k+1)}(1),$ since $y^{(k+1)}(1) = \beta \geq 0$.

Then also

$$\begin{aligned}
\mathscr{L}\psi^{\pm}(\chi) =&\mu^{(k)}(\chi)(\psi^{\pm}(\chi))'' + a^{(k)}(\chi)(\psi^{\pm}(\chi))' + b^{(k)}(\chi)\psi^{\pm}(\chi)\\
=&b^{(k)}(\chi)\left[\Theta^{-1}\|r^{(k)}\| + \max(|\phi_0|, |\beta|)\right] \pm \mathscr{L}y^{(k+1)}(\chi)\\
=&b^{(k)}(\chi)\left[\Theta^{-1}\|r^{(k)}\| + \max(|\phi_0|, |\beta|)\right] \pm r^{(k)}(\chi).
\end{aligned}$$

Since we have $b^{(k)}(\chi)\Theta^{-1} \leq -1, b^{(k)}(\chi) \leq -\Theta < 0$, using in the above inequality, we will get

$$\mathscr{L}\psi^{\pm}(\chi) \leq \left(-\|r\| \pm r^{(k)}(\chi)\right) + b^{(k)}(\chi)\max(|\phi_0|, |\beta|) \leq 0 \;\; \forall\, \chi \in (0,1),$$

where $\|r\| \geq r^{(k)}(\chi)$.

According to the minimal principle [27], it is evident that $\psi^{\pm}(\chi) \geq 0$ for all $\chi \in (0,1)$. Therefore, the desired estimate is satisfied.

Considering $y^{(k+1)}(\chi) = \mathcal{Y}(\chi)$, we show an approximation for the discrete solution, in the following lemma:

Lemma 4. Let $\mathcal{Y}(\chi) = (\mathcal{Y}_0)^{outer} + (\mathcal{Y}_0)^{inner}$ be the zeroth order estimation to the solution of equations (13) and (14). The term $(\mathcal{Y}_0)^{outer}$ represents the zeroth order estimation of the solution in the outer region, while $(\mathcal{Y}_0)^{inner}$ represents the zeroth order estimation in the boundary layer region. Following that, for a given positive integer j,

$$\lim_{h\to 0} \mathcal{Y}(jh) \approx (\mathcal{Y}_0)^{outer}(0) + (\phi(0) - (\mathcal{Y}_0)^{outer}(0))e^{-a^{(k)}(0)j\rho}, \text{ with } \rho = \frac{h}{\mu^{(k)}(0)}.$$

Proof. For $\epsilon = 0$, the reduced problem (13) is as follows:

$$a^{(k)}(\chi)\big((\mathcal{Y}_0)^{outer}(\chi)\big)' + b^{(k)}(\mathcal{Y}_0)^{outer}(\chi) = r^{(k)}(\chi), \quad (\mathcal{Y}_0)^{outer}(1) = \beta$$

and the boundary layer region problem is

$$\begin{aligned}&\big((\mathcal{Y}_0)^{inner}(\hat{\chi})\big)'' + a^{(k)}(0)\,\big((\mathcal{Y}_0)^{inner}(\hat{\chi})\big)' = 0,\\ &(\mathcal{Y}_0)^{inner}(0) = \phi_0 - (\mathcal{Y}_0)^{outer}(0), (\mathcal{Y}_0)^{inner}(\infty) = 0, \text{ where } \hat{\chi} = \frac{\chi}{\epsilon - \delta\mathscr{M}}.\end{aligned}$$

According to the theory of singular perturbations [28], the zeroth order asymptotic approximations to the problem's solution are

$$\mathcal{Y}(\chi) = (\mathcal{Y}_0)^{outer}(\chi) + \frac{a^{(k)}(0)}{a^{(k)}(\chi)}(\phi_0 - (\mathcal{Y}_0)^{outer}(0))e^{-\int\limits_0^{\chi}\frac{a^{(k)}(\chi)}{\mu^{(k)}(\chi)}d\chi}.$$

Given that the coefficients are locally constant on a small grid,

$$\mathcal{Y}(\chi) = (\mathcal{Y}_0)^{outer}(\chi) + (\phi_0 - (\mathcal{Y}_0)^{outer}(0))e^{-\frac{a^{(k)}(0)}{\mu^{(k)}(0)}\chi}$$

and hence, at the mesh points,

$$\begin{aligned}\mathcal{Y}(\chi_j) &= (\mathcal{Y}_0)^{outer}(\chi_j) + (\phi_0 - (\mathcal{Y}_0)^{outer}(0))e^{-\frac{a^{(k)}(0)}{\mu^{(k)}(0)}\chi_j}, \quad j = 0, 1, \ldots, N,\\ \mathcal{Y}(jh) &= (\mathcal{Y}_0)^{outer}(jh) + (\phi_0 - (\mathcal{Y}_0)^{outer}(0))e^{-\frac{a^{(k)}(0)}{\mu^{(k)}(0)}jh}.\end{aligned}$$

Therefore, $\lim\limits_{h\to 0}\mathcal{Y}(jh) = (\mathcal{Y}_0)^{outer}(0) + (\phi_0 - (\mathcal{Y}_0)^{outer}(0))e^{-a^{(k)}(0)j\rho}$ regarding $j = 0, 1, \ldots, N$, for $\rho = \frac{h}{\mu^{(k)}(0)}$.

3 Numerical schemes

We rewrite Eq.(13) as

$$\mu^{(k)}(\chi)y''^{(k+1)}(\chi) = g(\chi, y^{(k+1)}, y'^{(k+1)}) \tag{15}$$

$$\text{with } \; g(\chi, y^{(k+1)}, y'^{(k+1)}) = r^{(k)}(\chi) - a^{(k)}(\chi)y'^{(k+1)}(\chi) - b^{(k)}(\chi)y^{(k+1)}(\chi). \tag{16}$$

Now, we will partition the interval $[0, 1]$ into N equal segments with a constant mesh length h. This means that the mesh points $\chi_n = nh, \; n = 0, 1, 2, \ldots, N$.

3.1 Exponentially Fitted Higher Order Method-1 (EFHOM-1)

We use the finite difference technique proposed by Chawla [24] for solving the general non-linear boundary value problem, which may be expressed as $u'' = g(x, u, u')$.

$$\begin{aligned}\overline{u}'_s =& \frac{(u_{s+1} - u_{s-1})}{2h}, \; \overline{u}'_{s+1} = \frac{(3u_{s+1} - 4u_s - u_{s-1})}{2h}, \; \overline{u}'_{s-1} = \frac{(-u_{s+1} + 4u_s - 3u_{s-1})}{2h},\\ \overline{\overline{u}}'_s =& \overline{u}'_s - \frac{h}{20}(\overline{g}_{s+1} - \overline{g}_{s-1}), \; \frac{u_{s+1} - 2u_s + u_{s-1}}{h^2} = \frac{1}{12}\left(\overline{g}_{s+1} + 10\overline{\overline{g}}_s + \overline{g}_{s-1}\right),\end{aligned}$$

where $\overline{\overline{g}}_s = g(x_s, u_s, \overline{\overline{u}}')$ and $\overline{\overline{g}}_{s\pm1} = g(x_{s\pm1}, u_{s\pm1}, \overline{\overline{u}}'_{s\pm1})$.

Now, we introduce the fitting parameter $\sigma(\rho)$ for the second derivative and apply the preceding approach to equation (15), replacing $a^{(k)}(\chi)$, $b^{(k)}(\chi)$ and $r^{(k)}(\chi)$ for convenience, with $a(\chi)$, $b(\chi)$ and $r(\chi)$ respectively. In this context, we consider the initial approximation $y^{(0)}(\chi)$ as the solution to the reduced problem of (13)–(14). The succeeding approximations $\{y^{(k)}(\chi)\}_{k=0}^{\infty}$ are then determined by (15)–(16). We get the tridiagonal scheme

$$E_n y_{n-1}^{(k+1)} + F_n y_n^{(k+1)} + G_n y_{n+1}^{(k+1)} = H_n, \quad n = 1, 2, \ldots, N-1, \tag{17}$$

here

$$\begin{aligned}
E_n =& \mu_n\sigma_n + \frac{ha_{n+1}}{24} - \frac{5ha_n}{12} + \frac{h^2 a_n a_{n+1}}{48} + \frac{h^2 a_n a_{n-1}}{16} - \frac{h^3 a_n b_{n-1}}{24} - \frac{ha_{n-1}}{8} - \frac{h^2 b_{n-1}}{12},\\
F_n =& -2\mu_n\sigma_n - \frac{ha_{n+1}}{6} - \frac{h^2 a_n a_{n+1}}{12} - \frac{h^2 a_n a_{n-1}}{12} + \frac{5h^2 b_n}{6} + \frac{ha_{n-1}}{6},\\
G_n =& \mu_n\sigma_n + \frac{ha_{n+1}}{8} + \frac{h^2 b_{n+1}}{12} + \frac{5ha_n}{12} + \frac{h^2 a_n a_{n+1}}{16} + \frac{h^3 a_n b_{n+1}}{24} + \frac{h^2 a_n a_{n-1}}{48} - \frac{ha_{n-1}}{24},\\
H_n =& \frac{h^2}{12}\Big\{(1 - \frac{ha_n}{2})r_{n-1} + 10r_n + (1 + \frac{ha_n}{2})r_{n+1}\Big\}.
\end{aligned}$$

The tri-diagonal scheme mentioned above, which refers to EFHOM-1, together with the boundary conditions (14), is solved using the Thomas Algorithm. Applying Lemma 4, we obtain the fitting parameter: $\sigma(\rho) = \frac{a(0)\rho}{2}\coth\left(\frac{a(0)\rho}{2}\right)$. It represents a constant fitting parameter. Generally, we take the variable fitting parameter into account, i.e,

$$\sigma_n = \frac{a(\chi_n)\rho_n}{2}\coth\left(\frac{a(\chi_n)\rho_n}{2}\right), \quad \text{where} \quad \rho_n = \frac{h}{\mu_n}. \tag{18}$$

3.1.1 Convergence Analysis for EFHOM-1

Multiplying h both sides in the tridiagonal scheme (17) using boundary conditions, the system of equations is represented in matrix form as

$$(\mathbb{D} + \mathbb{J})\mathcal{W} + \mathcal{K} + \mathcal{T}(h) = 0, \tag{19}$$

here

$$\mathbb{D} = \left(\tfrac{\mu_n\sigma_n}{h}, \quad -\tfrac{\mu_n\sigma_n}{h}, \quad \tfrac{\mu_n\sigma_n}{h}\right) = \begin{pmatrix} \frac{-2\mu_1\sigma_1}{h} & \frac{\mu_1\sigma_1}{h} & 0 & \cdots & 0\\ \frac{\mu_2\sigma_2}{h} & \frac{-2\mu_2\sigma_2}{h} & \frac{\mu_2\sigma_2}{h} & \cdots & 0\\ 0 & . & . & \cdots & .\\ . & . & . & \cdots & .\\ 0 & \cdots & 0 & \frac{\mu_{N-1}\sigma_{N-1}}{h} & \frac{-2\mu_{N-1}\sigma_{N-1}}{h} \end{pmatrix},$$

$$\mathbb{J} = \left(\check{p}_m, \quad p_m, \quad \hat{p}_m\right) = \begin{pmatrix} p_1 & \hat{p}_1 & 0 & \cdots & 0\\ \check{p}_2 & p_2 & \hat{p}_2 & \cdots & 0\\ 0 & . & . & \cdots & .\\ . & . & . & \cdots & .\\ 0 & \cdots & 0 & \check{p}_{N-1} & p_{N-1} \end{pmatrix}, \quad \mathcal{T}(h) = O(h^4),$$

$$\check{p}_n = \frac{1}{12}\left[hb_{n-1} + \frac{a_{n+1}}{2} - 5a_n - \frac{h^2 a_n b_{n-1}}{2} - \frac{3a_{n-1}}{2} + \frac{ha_n(a_{n+1} + 3a_{n-1})}{4}\right],$$

$$p_n = \left[\frac{5hb_n}{6} - \frac{(a_{n+1} - a_{n-1})}{6} - \frac{ha_n(a_{n+1} + a_{n-1})}{12}\right],$$

$$\hat{p}_n = \frac{1}{12}\left[hb_{n+1} + \frac{3a_{n+1}}{2} + 5a_n + \frac{h^2 a_n b_{n+1}}{2} - \frac{a_{n-1}}{2} + \frac{ha_n(3a_{n+1}+a_{n-1})}{4}\right]$$

and

$$\mathcal{K} = \left[k_1 + \left(\frac{\mu_1\sigma_1}{h} + r_1\right)\phi_0, k_2, k_3, \ldots, k_{N-2}, k_{N-1} + \left(\frac{\mu_{N-1}\sigma_{N-1}}{h} + t_{N-1}\right)\beta\right]^T,$$

where

$$\mathcal{K}_n = -\frac{1}{12}\left[h(r_{n+1} + 10r_n + r_{n-1}) + \frac{h^2 a_n(r_{n+1} - r_{n-1})}{2}\right],\ n = 1, 2, \ldots, N-1.$$

Here, $\mathcal{W} = [\mathcal{W}_1, \mathcal{W}_2, \ldots, \mathcal{W}_{N-1}]^T$, the truncation errors occured at the mesh points $\mathcal{T}(h) = [\mathcal{T}_1, \mathcal{T}_2, \ldots, \mathcal{T}_{N-1}]^T$.

Let $W = [\overline{w}_1, \overline{w}_2, \ldots, \overline{w}_{N-1}]^T \cong \mathcal{Y}$ which at first fulfills the equation

$$(\mathbb{D} + \mathbb{J})\overline{w} + \mathcal{K} = 0. \tag{20}$$

Let $e_n = \overline{w}_n - \mathcal{W}_n$, $n = 1, 2, \ldots, N-1$ denote the discretization error. This will ensure that $\mathcal{E} = [e_1, e_2, \ldots, e_{N-1}]^T = \overline{w} - \mathcal{W}$.

Now subtracting (20) from (19), we get

$$(\mathbb{D} + \mathbb{J})\mathcal{E} = \mathcal{T}(h). \tag{21}$$

Considering $|a(\chi)| \le c_1$, $|b(\chi)| \le c_2$, for positive constants c_1, c_2 and $\mathbb{J}_{i,j}$, the $(i,j)^{th}$ element of the matrix $\mathbb{J}$, we have

$$\begin{aligned}
|\mathbb{J}_{n,n+1}| &= |\hat{p}_n| \le \frac{1}{12}\left(hc_2 + 6c_1 + \frac{h^2 c_1 c_2}{2} + hc_1^2\right),\\
|\mathbb{J}_{n,n-1}| &= |\check{p}_n| \le \frac{1}{12}\left(hc_2 - 6c_1 - \frac{h^2 c_1 c_2}{2} + hc_1^2\right).
\end{aligned}$$

For sufficiently small h, we have

$$\begin{aligned}
\frac{\mu_n\sigma_n}{h} + |\mathbb{J}_{n,n+1}| &\le \frac{c_1}{12}\left(\frac{\mu_n\sigma_n}{h} + 1\right) \ne 0,\ n = 1, 2, \ldots, N-2,\\
\frac{\mu_n\sigma_n}{h} + |\mathbb{J}_{n,n-1}| &\le \frac{c_1}{12}\left(\frac{\mu_n\sigma_n}{h} + 1\right) \ne 0,\ n = 1, 2, \ldots, N-1.
\end{aligned}$$

Therefore, the matrix is irreducible according to Varga's research [29], ensuring the stability and robustness of the numerical scheme (17).

Define $\mathcal{S}_n$ as the sum of the elements in the n^{th} row of the matrix $(\mathbb{D} + \mathbb{J})$, then we have

$$\begin{aligned}
\mathcal{S}_n &= -\frac{\mu_n\sigma_n}{h} + \frac{5hb_n}{6} - \frac{ha_{n+1}}{24} + \frac{5a_n}{12} + \frac{a_{n-1}}{8} + \frac{hb_{n+1}}{12} - \frac{ha_n a_{n+1}}{48} - \frac{ha_n a_{n-1}}{16} + \frac{h^2 a_n b_{n+1}}{24},\ n = 1,\\
\mathcal{S}_n &= -\frac{\mu_n\sigma_n}{h} + \frac{hb_{n-1}}{12} - \frac{a_{n+1}}{8} - \frac{5a_n}{12} + \frac{a_{n-1}}{24} - \frac{ha_n a_{n+1}}{16} - \frac{ha_n a_{n-1}}{48} - \frac{h^2 a_n b_{n-1}}{24} + \frac{5hb_n}{6},\ n = N-1,\\
\mathcal{S}_n &= \frac{h(b_{n-1} + 10b_n + b_{n+1})}{12} + \frac{h^2 a_n(b_{n+1} - b_{n-1})}{24}, \quad \text{for } n = 2\ ,3\ ,\ldots\ ,N-2.
\end{aligned}$$

Let $c_{1^*} = \min|a(\chi)|$, $c_1^* = \max|a(\chi)|$ and $c_{2^*} = \min|b(\chi)|$, $c_2^* = \max|b(\chi)|$, then $0 < c_{1^*} \le c_1 \le c_1^*$ and $0 < c_{2^*} \le c_2 \le c_2^*$.

It can be readily confirmed that the sum of $\mathbb{D}$ and $\mathbb{J}$, denoted as $(\mathbb{D} + \mathbb{J})$, exhibits monotonic behavior, as stated in references [29] and [30].

From this $(\mathbb{D}+\mathbb{J})^{-1}$ exists because $(\mathbb{D}+\mathbb{J})^{-1}\geq 0$. Based on the error equation (21), we deduce that
$$||\mathcal{E}|| = ||(\mathbb{D}+\mathbb{J})^{-1}||\cdot||\mathcal{T}||.$$
When h is small enough, we have
$$\begin{aligned}&\mathcal{S}_n > \frac{h^2}{24}c_1c_2 \quad \text{for} \quad n=1, N-1 \quad \text{and}\\ &\mathcal{S}_n > \frac{h^2}{24}c_1c \quad \text{for} \quad n=2,3,\ldots,N-2, \text{ where } c=|b_{n+1}-b_{n-1}|.\end{aligned} \tag{22}$$

Let consider $(\mathbb{D}+\mathbb{J})^{-1}_{(n,i)}$ be the $(n,i)^{th}$ element of $(\mathbb{D}+\mathbb{J})^{-1}$ and we define
$$||(\mathbb{D}+\mathbb{J})^{-1}|| = \max_{1\leq n\leq N-1}\sum_{i=1}^{N-1}(\mathbb{D}+\mathbb{J})^{-1}_{n,i} \quad \text{and} \quad ||\mathcal{T}(h)|| = \max_{1\leq n\leq N-1}|\mathcal{T}_n|,$$

since $(\mathbb{D}+\mathbb{J})^{-1}_{(n,i)}\geq 0$ and $\sum\limits_{i=1}^{N-1}(\mathbb{D}+\mathbb{J})^{-1}_{(n,i)}\cdot\mathcal{S}_i = 1$ for $n=1,2,\ldots,N-1$.

One has $(\mathbb{D}+\mathbb{J})^{-1}_{(n,1)} \leq \frac{1}{\mathcal{S}_1}\leq \frac{24}{h^2c_1c_2^2}$ and $(\mathbb{D}+\mathbb{J})^{-1}_{(n,N-1)} \leq \frac{1}{\mathcal{S}_{N-1}}\leq \frac{24}{h^2c_1c_2^2}$.

Additionally $\sum\limits_{i=2}^{N-2}(\mathbb{D}+\mathbb{J})^{-1}_{(n,i)} \leq \frac{1}{\min\limits_{2\leq i\leq N-2}\mathcal{S}_i}\leq \frac{24}{h^2c_1c}$ for $n=1,2,\ldots,N-1$.

So, using equations (21) and (22), we get
$$||\mathcal{E}|| = \frac{24}{h^2}\left[\frac{1}{c_1c_2}+\frac{1}{cc_1}+\frac{1}{c_1c_2}\right]\times O(h^4) = O(h^2).$$
This demonstrates the convergence of the finite difference scheme (17).

3.2 Exponentially Fitted Higher Order Method-2 (EFHOM-2)

In this section, we consider the finite difference method proposed by Chawla [25] for the general nonlinear boundary value problem of the form $w''=g(x,w,w')$, as illustrated below:
$$\overline{w}'_s = \frac{1}{2h}[w_{s+1}-w_{s-1}], \quad \overline{w}'_{s+1} = \frac{1}{2h}[3w_{s+1}-4w_s+w_{s-1}], \quad \overline{w}'_{s-1} = \frac{1}{2h}[-w_{s+1}+4w_s-3w_{s-1}],$$
$$\overline{\overline{w}}'_{s+1} = \frac{1}{2h}[w_{s+1}-w_{s-1}]+\frac{h}{3}[2\overline{g}_s+\overline{g}_{s+1}], \quad \overline{\overline{w}}'_{s-1} = \frac{1}{2h}[w_{s+1}-w_{s-1}]-\frac{h}{3}[2\overline{g}_s+\overline{g}_{s-1}],$$
$$\overline{w}_{s+\frac{1}{2}} = \frac{1}{32}[15w_{s+1}+18w_s-w_{s-1}]-\frac{h^2}{64}[3\overline{g}_{s+1}+4\overline{g}_s-\overline{g}_{s-1}],$$
$$\overline{w}_{s-\frac{1}{2}} = \frac{1}{32}[-w_{s+1}+18w_s+15w_{s-1}]-\frac{h^2}{64}[-\overline{g}_{s+1}+4\overline{g}_s+3\overline{g}_{s-1}],$$
$$\overline{\overline{w}}'_{s+\frac{1}{2}} = \frac{1}{4h}[5w_{s+1}-6w_s+w_{s-1}]-\frac{h}{48}[3\overline{g}_{s+1}+8\overline{g}_s+\overline{g}_{s-1}],$$
$$\overline{\overline{w}}'_{s-\frac{1}{2}} = \frac{1}{4h}[-w_{s+1}+6w_s-5w_{s-1}]-\frac{h}{48}[\overline{g}_{s+1}+8\overline{g}_s+3\overline{g}_{s-1}],$$
$$\hat{w}'_s = \overline{w}'_s + h\left[\frac{1}{78}(\overline{g}_{s+1}-\overline{g}_{s-1})-\frac{1}{52}(\overline{\overline{g}}_{s+1}-\overline{\overline{g}}_{s-1})-\frac{2}{13}(\overline{\overline{g}}_{s+\frac{1}{2}}-\overline{\overline{g}}_{s-\frac{1}{2}})\right],$$
$$[w_{s-1}-2w_s+w_{s+1}] = \frac{h^2}{60}\left[26\hat{g}_s+\overline{\overline{g}}_{s+1}+\overline{\overline{g}}_{s-1}+16(\overline{\overline{g}}_{s+\frac{1}{2}}+\overline{\overline{g}}_{s-\frac{1}{2}})\right],$$

where

$$\overline{\overline{g}}_{s\pm1} = g(x_{s\pm1}, w_{s\pm1}, \overline{\overline{w}}'_{s\pm1}), \quad \overline{\overline{g}}_{s\pm\frac{1}{2}} = g(x_{s\pm\frac{1}{2}}, w_{s\pm\frac{1}{2}}, \overline{\overline{w}}'_{s\pm\frac{1}{2}}), \quad \hat{g}_s = g(x_s, w_s, \hat{w}'_s).$$

Now, we introduce the fitting parameter $\sigma(\rho)$ to represent the second derivative and then apply the previously described approach to equation (15). The solution of the simplified problem of (13)–(14) is considered to be the initial approximation $y^{(0)}(\chi)$, and the succeeding approximations $\{y^{(k)}(\chi)\}_{k=0}^{\infty}$ are determined by (15)–(16). We will get the tridiagonal scheme

$$E_n y_{n-1}^{(k+1)} + F_n y_n^{(k+1)} + G_n y_{n+1}^{(k+1)} = H_n, \quad n = 1, 2, \ldots, N-1, \tag{23}$$

where

$$\begin{aligned}
E_n =& \mu_n\sigma_n + \frac{ha_{n+1/2}}{15} - \frac{ha_{n+1}}{120} - \frac{ha_{n-1/2}}{3} - \frac{ha_{n-1}}{120} + \frac{h^2b_{n-1}}{60} + \frac{h^2b_{n-1/2}}{8} - \frac{h^2b_{n+1/2}}{120} - \frac{13ha_n}{60} \\
&- \frac{h^2a_{n-1}^2}{120} - \frac{h^2a_{n+1}^2}{360} - \frac{7h^2a_{n-1}a_n}{720} - \frac{h^2a_{n+1}a_n}{720} + \frac{19h^2a_{n-1/2}a_n}{180} - \frac{h^2a_{n+1/2}a_n}{180} - \frac{h^3b_{n-1}a_n}{360} \\
&- \frac{19h^3b_{n-1/2}a_n}{480} - \frac{h^3b_{n+1/2}a_n}{96} + \frac{h^2a_{n-1}a_{n-1/2}}{40} - \frac{h^2a_{n-1}a_{n+1/2}}{120} - \frac{h^2a_{n+1}a_{n-1/2}}{360} \\
&+ \frac{h^2a_{n+1}a_{n+1/2}}{120} + \frac{h^3a_{n-1}a_n^2}{360} + \frac{h^3a_{n+1}a_n^2}{360} + \frac{h^3a_{n-1}^2a_n}{240} - \frac{h^3a_{n+1}^2a_n}{720} - \frac{h^3a_{n-1/2}a_n^2}{180} \\
&- \frac{h^3a_{n+1/2}a_n^2}{180} + \frac{h^3a_{n-1}b_{n-1}}{180} - \frac{3h^3a_{n-1}b_{n-1/2}}{160} + \frac{h^3a_{n-1}b_{n+1/2}}{160} - \frac{h^3a_{n+1}b_{n-1/2}}{480} \\
&+ \frac{h^3a_{n+1}b_{n+1/2}}{160} - \frac{h^3a_{n-1/2}b_{n-1}}{60} + \frac{h^3a_{n+1/2}b_{n-1}}{180} + \frac{h^4b_{n-1/2}a_n^2}{480} - \frac{h^4b_{n+1/2}a_n^2}{480} \\
&+ \frac{h^4b_{n-1}b_{n-1/2}}{80} - \frac{h^4b_{n-1}b_{n+1/2}}{240} - \frac{h^3a_{n-1}a_{n-1/2}a_n}{160} - \frac{h^3a_{n-1}a_{n+1/2}a_n}{480} + \frac{h^3a_{n+1}a_{n-1/2}a_n}{1440} \\
&+ \frac{h^3a_{n+1}a_{n+1/2}a_n}{480} - \frac{h^4a_{n-1}b_{n-1}a_n}{360} + \frac{3h^4a_{n-1}b_{n-1/2}a_n}{640} + \frac{h^4a_{n-1}b_{n+1/2}a_n}{640} + \frac{h^4a_{n+1}b_{n-1/2}a_n}{1920} \\
&+ \frac{h^4a_{n+1}b_{n+1/2}a_n}{640} + \frac{h^4a_{n-1/2}b_{n-1}a_n}{240} + \frac{h^4a_{n+1/2}b_{n-1}a_n}{720} - \frac{h^5b_{n-1}b_{n-1/2}a_n}{320} - \frac{h^5b_{n-1}b_{n+1/2}a_n}{960},
\end{aligned}$$

$$\begin{aligned}
F_n =& -2\mu_n\sigma_n + \frac{2ha_{n-1/2}}{5} - \frac{2ha_{n+1/2}}{5} + \frac{13h^2b_n}{30} + \frac{3h^2b_{n-1/2}}{20} + \frac{3h^2b_{n+1/2}}{20} + \frac{h^2a_{n-1}^2}{90} + \frac{h^2a_{n+1}^2}{90} \\
&+ \frac{h^2a_{n-1}a_n}{90} + \frac{h^2a_{n+1}a_n}{90} - \frac{h^2a_{n-1/2}a_n}{10} - \frac{h^2a_{n+1/2}a_n}{10} + \frac{h^3a_{n-1}b_n}{90} - \frac{h^3a_{n+1}b_n}{90} - \frac{2h^3a_{n-1/2}b_n}{45} \\
&+ \frac{2h^3a_{n+1/2}b_n}{45} - \frac{3h^3b_{n-1/2}a_n}{80} + \frac{3h^3b_{n+1/2}b_n}{80} + \frac{h^4b_{n-1/2}b_n}{60} + \frac{h^4b_{n+1/2}b_n}{60} - \frac{h^2a_{n-1}a_{n-1/2}}{30} \\
&+ \frac{h^2a_{n-1}a_{n+1/2}}{90} + \frac{h^2a_{n+1}a_{n-1/2}}{90} - \frac{h^2a_{n+1}a_{n+1/2}}{30} - \frac{h^3a_{n-1}^2a_n}{180} + \frac{h^3a_{n+1}^2a_n}{180} + \frac{h^3a_{n-1}b_{n-1/2}}{40} \\
&- \frac{h^3a_{n-1}b_{n+1/2}}{120} + \frac{h^3a_{n+1}b_{n-1/2}}{120} - \frac{h^3a_{n+1}b_{n+1/2}}{40} - \frac{h^4a_{n-1}a_nb_n}{180} - \frac{h^4a_{n+1}a_nb_n}{180} + \frac{h^4a_{n-1/2}a_nb_n}{90} \\
&+ \frac{h^4a_{n+1/2}a_nb_n}{90} - \frac{h^5b_{n-1/2}a_nb_n}{240} + \frac{h^5b_{n+1/2}a_nb_n}{240} + \frac{h^3a_{n-1}a_{n-1/2}a_n}{120} + \frac{h^3a_{n-1}a_{n+1/2}a_n}{360} \\
&- \frac{h^3a_{n+1}a_{n-1/2}a_n}{360} - \frac{h^3a_{n+1}a_{n+1/2}a_n}{120} - \frac{h^4a_{n-1}b_{n-1/2}a_n}{160} - \frac{h^4a_{n-1}b_{n+1/2}a_n}{480} - \frac{h^4a_{n+1}b_{n-1/2}a_n}{480} \\
&- \frac{h^4a_{n+1}b_{n+1/2}a_n}{160},
\end{aligned}$$

$$
\begin{aligned}
G_n =&\mu_n\sigma_n + \frac{ha_{n-1}}{120} + \frac{ha_{n+1}}{120} - \frac{ha_{n-1/2}}{15} + \frac{ha_{n+1/2}}{3} + \frac{h^2b_{n+1}}{60} - \frac{h^2b_{n-1/2}}{120} + \frac{h^2b_{n+1/2}}{8} + \frac{13ha_n}{60} \\
&- \frac{h^2a_{n-1}^2}{360} - \frac{h^2a_{n+1}^2}{120} - \frac{h^2a_{n-1}a_n}{720} - \frac{7h^2a_{n+1}a_n}{720} - \frac{h^2a_{n-1/2}a_n}{180} + \frac{19h^2a_{n+1/2}a_n}{180} + \frac{h^3b_{n+1}a_n}{360} \\
&+ \frac{h^3b_{n-1/2}a_n}{96} + \frac{19h^3b_{n+1/2}a_n}{480} + \frac{h^2a_{n-1}a_{n-1/2}}{120} - \frac{h^2a_{n-1}a_{n+1/2}}{360} - \frac{h^2a_{n+1}a_{n-1/2}}{120} \\
&+ \frac{h^2a_{n+1}a_{n+1/2}}{40} - \frac{h^3a_{n-1}a_n^2}{360} - \frac{h^3a_{n+1}a_n^2}{360} + \frac{h^3a_{n-1}^2a_n}{720} - \frac{h^3a_{n+1}^2a_n}{240} + \frac{h^3a_{n-1/2}a_n^2}{180} \\
&+ \frac{h^3a_{n+1/2}a_n^2}{180} - \frac{h^3a_{n+1}b_{n+1}}{180} - \frac{h^3a_{n-1}b_{n-1/2}}{160} + \frac{h^3a_{n-1}b_{n+1/2}}{480} - \frac{h^3a_{n+1}b_{n-1/2}}{160} \\
&+ \frac{3h^3a_{n+1}b_{n+1/2}}{160} - \frac{h^3a_{n-1/2}b_{n+1}}{180} + \frac{h^3a_{n+1/2}b_{n+1}}{60} - \frac{h^4b_{n-1/2}a_n^2}{480} + \frac{h^4b_{n+1/2}a_n^2}{480} \\
&- \frac{h^4b_{n+1}b_{n-1/2}}{240} + \frac{h^4b_{n+1}b_{n+1/2}}{80} - \frac{h^3a_{n-1}a_{n-1/2}a_n}{480} - \frac{h^3a_{n-1}a_{n+1/2}a_n}{1440} + \frac{h^3a_{n+1}a_{n-1/2}a_n}{480} \\
&+ \frac{h^3a_{n+1}a_{n+1/2}a_n}{160} - \frac{h^4a_{n+1}b_{n+1}a_n}{360} + \frac{h^4a_{n-1}b_{n-1/2}a_n}{640} + \frac{h^4a_{n-1}b_{n+1/2}a_n}{1920} + \frac{h^4a_{n+1}b_{n-1/2}a_n}{640} \\
&+ \frac{3h^4a_{n+1}b_{n+1/2}a_n}{640} + \frac{h^4a_{n-1/2}b_{n+1}a_n}{720} + \frac{h^4a_{n+1/2}b_{n+1}a_n}{240} + \frac{h^5b_{n+1}b_{n-1/2}a_n}{960} + \frac{h^5b_{n+1}b_{n+1/2}a_n}{320},
\end{aligned}
$$

and

$$
\begin{aligned}
H_n =&\frac{13h^2r_n}{30} + \frac{h^2r_{n-1}}{60} + \frac{h^2r_{n+1}}{60} + \frac{4h^2r_{n-1/2}}{15} + \frac{4h^2r_{n+1/2}}{15} + \frac{h^3a_{n-1}r_n}{90} - \frac{h^3a_{n+1}r_n}{90} - \frac{h^3r_{n-1}a_n}{360} \\
&+ \frac{h^3r_{n+1}a_n}{360} - \frac{2h^3a_{n-1/2}r_n}{45} + \frac{2h^3a_{n+1/2}r_n}{45} - \frac{h^3r_{n-1/2}a_n}{15} + \frac{h^3r_{n+1/2}a_n}{15} + \frac{h^4b_{n-1/2}r_n}{60} \\
&+ \frac{h^4b_{n+1/2}r_n}{60} + \frac{h^3a_{n-1}r_{n-1}}{180} - \frac{h^3a_{n+1}r_{n+1}}{180} - \frac{h^3a_{n-1/2}r_{n-1}}{60} - \frac{h^3a_{n-1/2}r_{n+1}}{180} + \frac{h^3a_{n+1/2}r_{n-1}}{180} \\
&+ \frac{h^3a_{n+1/2}r_{n+1}}{60} + \frac{h^4b_{n-1/2}r_{n-1}}{80} - \frac{h^4b_{n-1/2}r_{n+1}}{240} - \frac{h^4b_{n+1/2}r_{n-1}}{240} + \frac{h^4b_{n+1/2}r_{n+1}}{80} - \frac{h^4a_{n-1}a_nr_n}{180} \\
&- \frac{h^4a_{n+1}a_nr_n}{180} + \frac{h^4a_{n-1/2}a_nr_n}{90} + \frac{h^4a_{n+1/2}a_nr_n}{90} - \frac{h^5b_{n-1/2}a_nr_n}{240} + \frac{h^5b_{n+1/2}a_nr_n}{240} - \frac{h^4a_{n-1}r_{n-1}a_n}{360} \\
&- \frac{h^4a_{n+1}r_{n+1}a_n}{360} + \frac{h^4a_{n-1/2}r_{n-1}a_n}{240} + \frac{h^4a_{n-1/2}r_{n+1}a_n}{720} + \frac{h^4a_{n+1/2}r_{n-1}a_n}{720} + \frac{h^4a_{n+1/2}r_{n+1}a_n}{240} \\
&- \frac{h^5b_{n-1/2}r_{n-1}a_n}{320} + \frac{h^5b_{n-1/2}r_{n+1}a_n}{960} - \frac{h^5b_{n+1/2}r_{n-1}a_n}{960} + \frac{h^5b_{n+1/2}r_{n+1}b_n}{320}.
\end{aligned}
$$

The tri-diagonal scheme mentioned above, which refers to EFHOM-2, when combined with the boundary conditions (14), is solved using the Thomas Algorithm. Here, we also employ lemma 4 to determine the fitting parameter, which is equivalent to equation (18).

Note. Similar to Section 3.1.1, the convergence of the finite difference scheme (23) can be demonstrated and proved to be of second order.

4 Numerical results

To test the efficiency of EFHOM-1 and EFHOM-2, we have applied them to two nonlinear singularly perturbed differential-difference equations with small negative shift.

Given that the precise solutions for these problems are not known for various values of δ, the maximum absolute errors for the test problems are determined using the double mesh approach as follows:

$$E_N = \max_{0\le n\le N} |y_n^N - y_{2n}^{2N}|.$$

The numerical rate of convergence for both examples has been calculated by the formula

$$R_N = \frac{log|E_N/E_{2N}|}{log2}.$$

Example 1. $\epsilon y''(\chi) + 2y'(\chi - \delta) - e^{y(\chi)} = 0$, along with the interval and boundary conditions $y(\chi) = 0,\ -\delta \le \chi \le 0,\ y(1) = 0.$

The sequence of linear equations obtained by applying quasilnearization technique is given by the following recurrence relation

$$\epsilon {y''}^{(k+1)}(\chi) + 2{y'}^{(k+1)}(\chi - \delta) - e^{y^{(k)}} y^{(k+1)}(\chi) = e^{y^{(k)}}(1 - y^{(k)}),$$

with the interval and boundary conditions $y^{(k+1)}(\chi) = 0,\ -\delta \le \chi \le 0,\ y^{(k+1)}(1) = 0.$

Example 2. $\epsilon y''(\chi) + y(\chi)y'(\chi - \delta) - y(\chi) = 0$, along with the interval and boundary conditions $y(\chi) = 1,\ -\delta \le \chi \le 0,\ y(1) = 1.$

The sequence of linear equations obtained by applying quasilnearization technique is given by the following recurrence relation

$$\epsilon {y''}^{(k+1)}(\chi) + y^{(k)}(\chi){y'}^{(k+1)}(\chi - \delta) + (-1 + {y'}^{(k)}(\chi - \delta))y^{(k+1)}(\chi) = y^{(k)}(\chi){y'}^{(k)}(\chi - \delta),$$

with the interval and boundary conditions $y^{(k+1)}(\chi) = 1,\ -\delta \le \chi \le 0,\ \ y^{(k+1)}(1) = 1.$

5 *Conclusion*

In this paper, higher order fitted finite difference methods EFHOM-1 and EFHOM-2 are presented for singularly perturbed nonlinear differential-difference equation with small negative shift.

The quasilinearization approach is utilized to transform the nonlinear problem into a series of linear problems. Higher order fitted finite difference methods are applied to this sequence of linear problems. It is theoretically proved that for all values of ϵ, the methods presented are uniformly convergent with order 2.

The maximum absolute errors and the numerical rates of convergence for the solutions of the problems 1 and 2 are calculated by the numerical schemes given in Section 3.1 and Section 3.2 and are tabulated in Tables 1–4. The results in Tables 1 and 2 are compared with [3] and [4] respectively and are found to be in good agreement. The impact of a shift on the problem's solution's layer behavior is shown in Figures 1–4 obtained by the numerical method given in Section 3.1 and Section 3.2. The graphical illustrations described in [4] also reveal similar boundary layer behavior to that depicted in the present paper. The log-log plot of maximum point-wise errors for Examples 1 and 2 using the methods EFHOM-1 and EFHOM-2 are plotted in Figures (5-6) respectively. These graphs illustrate the decay of the maximum absolute errors as the number of mesh points increases, thereby demonstrating the convergence of the proposed methods.

The effectiveness of the proposed methods and the implications of the shifts on the solution's layer behavior are both investigated. The present method offers significant advantages for solving the nonlinear singularly perturbed differential-difference equations based on the comprehensive numerical work on both examples.

Table 1

Maximum absolute errors E_N for Example 1 with $\delta = 0.4\epsilon$

$\epsilon \downarrow N \rightarrow$	100	200	300	400	500
EFHOM-1					
10^{-2}	8.8642E-04	3.9927E-04	2.2482E-04	1.4085E-04	9.4522E-05
10^{-3}	8.9469E-04	4.4893E-04	2.9964E-04	2.2486E-04	1.7994E-04
10^{-4}	8.9469E-04	4.4893E-04	2.9964E-04	2.2486E-04	1.7995E-04
10^{-5}	8.9469E-04	4.4893E-04	2.9964E-04	2.2486E-04	1.7995E-04
10^{-6}	8.9469E-04	4.4893E-04	2.9964E-04	2.2486E-04	1.7995E-04
10^{-7}	8.9469E-04	4.4893E-04	2.9964E-04	2.2486E-04	1.7995E-04
10^{-8}	8.9469E-04	4.4893E-04	2.9964E-04	2.2486E-04	1.7995E-04
10^{-9}	8.9469E-04	4.4893E-04	2.9964E-04	2.2486E-04	1.7995E-04
10^{-10}	8.9469E-04	4.4893E-04	2.9964E-04	2.2486E-04	1.7995E-04
E_N	8.9469E-04	4.4893E-04	2.9964E-04	2.2486E-04	1.7995E-04
EFHOM-2					
10^{-2}	9.5217E-04	4.2995E-04	2.4284E-04	1.5255E-04	1.0260E-04
10^{-3}	9.6088E-04	4.8237E-04	3.2201E-04	2.4167E-04	1.9340E-04
10^{-4}	9.6088E-04	4.8237E-04	3.2201E-04	2.4167E-04	1.9341E-04
10^{-5}	9.6088E-04	4.8237E-04	3.2201E-04	2.4167E-04	1.9341E-04
10^{-6}	9.6088E-04	4.8237E-04	3.2201E-04	2.4167E-04	1.9341E-04
10^{-7}	9.6088E-04	4.8237E-04	3.2201E-04	2.4167E-04	1.9341E-04
10^{-8}	9.6088E-04	4.8237E-04	3.2201E-04	2.4167E-04	1.9341E-04
10^{-9}	9.6088E-04	4.8237E-04	3.2201E-04	2.4167E-04	1.9341E-04
10^{-10}	9.6088E-04	4.8237E-04	3.2201E-04	2.4167E-04	1.9341E-04
E_N	9.6088E-04	4.8237E-04	3.2201E-04	2.4167E-04	1.9341E-04
Results in [3] for $\epsilon \in \{10^{-1}, 10^{-2}, \ldots, 10^{-8}\}$					
$N \rightarrow$	64	128	256	512	1024
E_N	5.655E-02	1.725E-02	5.420E-03	1.645E-03	4.817E-04

Table 2

Maximum absolute errors E_N for Example 2 with $\delta = 0.5\epsilon$

$\epsilon \downarrow N \rightarrow$	100	200	300	400	500
EFHOM-1					
2^{-2}	2.4910E-05	6.2125E-06	2.7599E-06	1.5522E-06	9.9333E-07
2^{-4}	8.2732E-05	2.0085E-05	8.8775E-06	4.9840E-06	3.1869E-06
2^{-6}	4.6993E-04	8.3055E-05	3.5223E-05	1.9452E-05	1.2280E-05
2^{-8}	2.1723E-03	6.0716E-04	2.3510E-04	1.1519E-04	6.5517E-05
2^{-10}	2.4798E-03	1.2370E-03	7.9298E-04	5.4352E-04	3.8222E-04
2^{-12}	2.4799E-03	1.2449E-03	8.3108E-04	6.2371E-04	4.9905E-04
2^{-14}	2.4799E-03	1.2449E-03	8.3108E-04	6.2373E-04	4.9919E-04
2^{-16}	2.4799E-03	1.2449E-03	8.3108E-04	6.2373E-04	4.9919E-04
2^{-18}	2.4799E-03	1.2449E-03	8.3108E-04	6.2373E-04	4.9919E-04
2^{-20}	2.4799E-03	1.2449E-03	8.3108E-04	6.2373E-04	4.9919E-04
E_N	2.4799E-03	1.2449E-03	8.3108E-04	6.2373E-04	4.9919E-04
EFHOM-2					
2^{-2}	3.5710E-05	8.9102E-06	3.9587E-06	2.2265E-06	1.4249E-06
2^{-4}	1.2693E-04	3.1031E-05	1.3734E-05	7.7141E-06	4.9337E-06
2^{-6}	6.7116E-04	1.2730E-04	5.4967E-05	3.0569E-05	1.9363E-05
2^{-8}	2.6279E-03	7.8308E-04	3.2323E-04	1.6559E-04	9.6959E-05
2^{-10}	2.9723E-03	1.4836E-03	9.5342E-04	6.5845E-04	4.6894E-04
2^{-12}	2.9724E-03	1.4931E-03	9.9691E-04	7.4823E-04	5.9872E-04
2^{-14}	2.9724E-03	1.4931E-03	9.9691E-04	7.4826E-04	5.9889E-04
2^{-16}	2.9724E-03	1.4931E-03	9.9691E-04	7.4826E-04	5.9889E-04
2^{-18}	2.9724E-03	1.4931E-03	9.9691E-04	7.4826E-04	5.9889E-04
2^{-20}	2.9724E-03	1.4931E-03	9.9691E-04	7.4826E-04	5.9889E-04
E_N	2.9724E-03	1.4931E-03	9.9691E-04	7.4826E-04	5.9889E-04
Results in [4] for $\epsilon \in \{2^{-1}, 2^{-2}, \ldots, 2^{-32}\}$					
$N \rightarrow$	32	64	128	256	512
E_N	4.84E-02	8.33E-03	1.87E-03	4.45E-03	1.09E-04

Table 3

The numerical rate of convergence R_N for the Example 1 for different values of δ with $\epsilon = 0.01$

$\delta \downarrow N \rightarrow$	100	200	300	400	500
EFHOM-1					
10^{-3}	1.9332	2.1167	1.9830	2.0290	2.0017
10^{-4}	2.0592	2.0810	2.0335	2.0081	2.0124
10^{-5}	2.0703	2.0783	2.0325	2.0025	2.0120
10^{-6}	2.0713	2.0781	2.0324	2.0020	2.0120
10^{-7}	2.0715	2.0781	2.0324	2.0019	2.0120
10^{-8}	2.0715	2.0781	2.0324	2.0019	2.0120
10^{-9}	2.0715	2.0781	2.0324	2.0019	2.0120
10^{-10}	2.0715	2.0781	2.0324	2.0019	2.0120
EFHOM-2					
10^{-3}	1.9237	2.1207	1.9919	2.0301	2.0069
10^{-4}	2.0504	2.0835	2.0321	2.0135	2.0129
10^{-5}	2.0616	2.0808	2.0338	2.0077	2.0125
10^{-6}	2.0627	2.0805	2.0337	2.0072	2.0124
10^{-7}	2.0628	2.0805	2.0337	2.0071	2.0124
10^{-8}	2.0628	2.0805	2.0337	2.0071	2.0124
10^{-9}	2.0628	2.0805	2.0337	2.0071	2.0124
10^{-10}	2.0628	2.0805	2.0337	2.0071	2.0124

Table 4

The numerical rate of convergence R_N for the Example 2 for different values of δ with $\epsilon = 0.01$

$\delta \downarrow N \rightarrow$	100	200	300	400	500
EFHOM-1					
10^{-3}	2.2226	2.0594	2.0199	2.0053	2.0015
10^{-4}	2.1767	2.0464	2.0208	2.0118	2.0075
10^{-5}	2.1729	2.0454	2.0204	2.0115	2.0074
10^{-6}	2.1725	2.0453	2.0203	2.0115	2.0073
10^{-7}	2.1725	2.0453	2.0203	2.0115	2.0073
10^{-8}	2.1725	2.0453	2.0203	2.0115	2.0073
10^{-9}	2.1725	2.0453	2.0203	2.0115	2.0073
10^{-10}	2.1725	2.0453	2.0203	2.0115	2.0073
EFHOM-2					
10^{-3}	2.2026	2.0536	2.0172	2.0037	2.0006
10^{-4}	2.1622	2.0424	2.0190	2.0107	2.0069
10^{-5}	2.1589	2.0414	2.0186	2.0105	2.0067
10^{-6}	2.1585	2.0414	2.0185	2.0105	2.0067
10^{-7}	2.1585	2.0413	2.0185	2.0105	2.0067
10^{-8}	2.1585	2.0413	2.0185	2.0105	2.0067
10^{-9}	2.1585	2.0413	2.0185	2.0105	2.0067
10^{-10}	2.1585	2.0413	2.0185	2.0105	2.0067

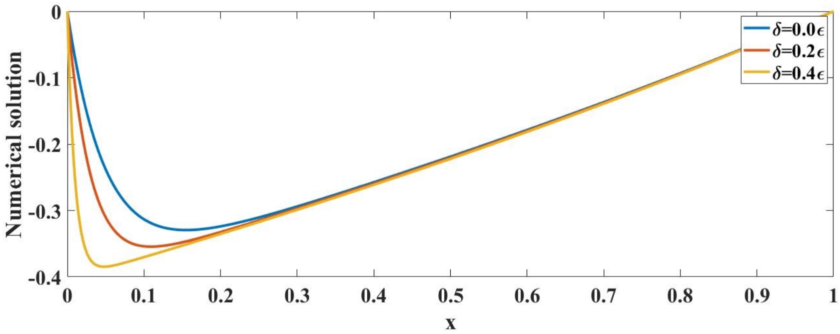

Figure 1. Numerical solution for the given example 1 when $\epsilon = 0.1$ in EFHOM-1 (3.1)

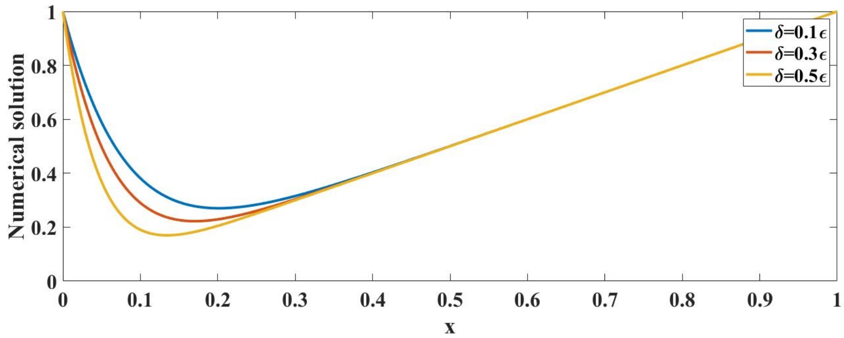

Figure 2. Numerical solution for the given example 2 when $\epsilon = 0.1$ in EFHOM-1 (3.1)

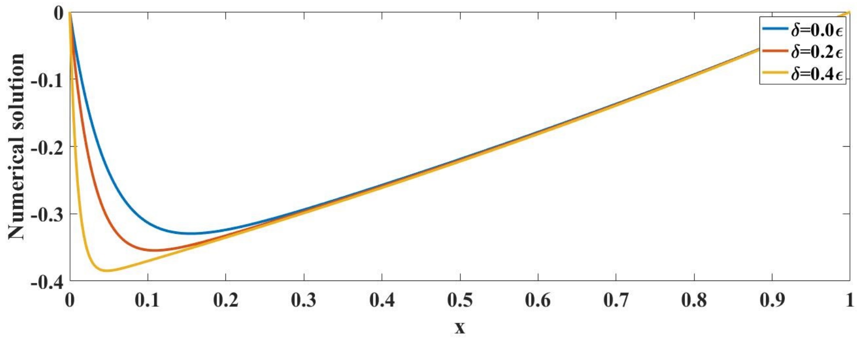

Figure 3. Numerical solution for the given example 1 when $\epsilon = 0.1$ in EFHOM-2 (3.2)

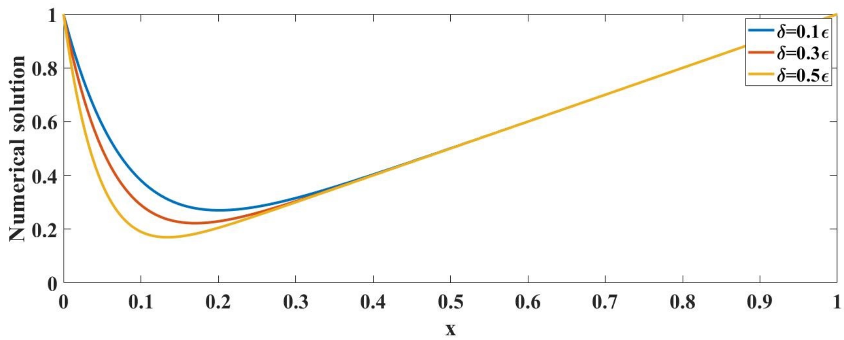

Figure 4. Numerical solution for the given example 2 when $\epsilon = 0.1$ in EFHOM-2 (3.2)

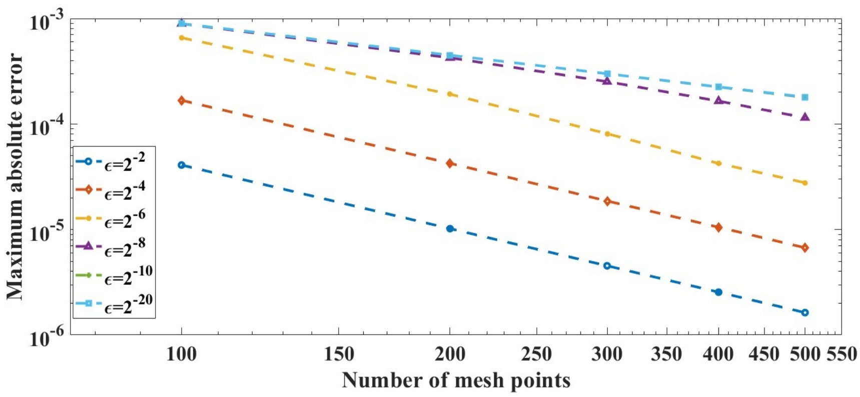

Figure 5. Log-log plot for Example 1 in EFHOM-1 (3.1)

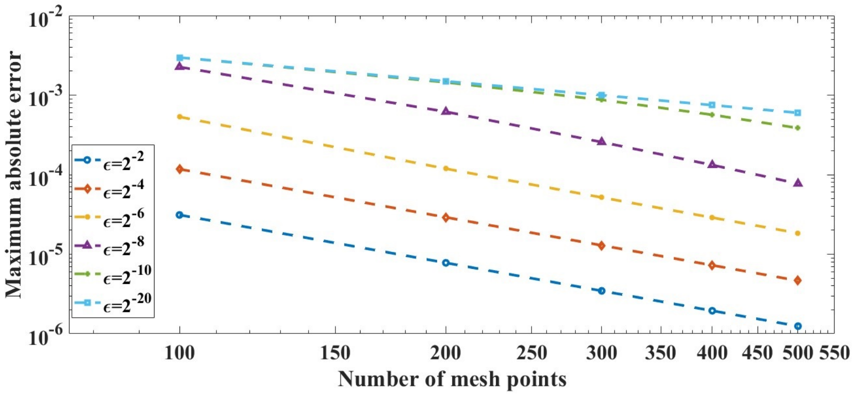

Figure 6. Log-log plot for Example 2 in EFHOM-2 (3.2)

Acknowledgments

The authors express their gratitude to the National Board for Higher Mathematics, Department of Atomic Energy, Government of India, for providing financial assistance through project No. 02011/8/2021 NBHM(R.P)/R&D II/7224, dated 24.06.2021.

Authors' contributions

The authors contributed equally to this work.

Conflict of Interest

The authors declare no conflict of interest.

References

1 Chang, K.V., & Howes, F.A. (1984). *Nonlinear Singular Perturbation Phenomena: Theory and Applications.* Springer-Verlag, New York. https://doi.org/10.1007/978-1-4612-1114-3

2 Lange, C.G., & Miura, R.M. (1991). Singular Perturbation Analysis of Boundary Value Problems for Differential-Difference Equations. IV. A Nonlinear Example with Layer Behavior. *Studies in Applied Mathematics, 84*(3), 231–273. https://doi.org/10.1002/sapm1991843231

3 Kadalbajoo, M.K., & Kumar, D. (2010). A computational method for singularly perturbed nonlinear differential-difference equations with small shift. *Applied Mathematical Modelling, 34*(9), 2584–2596. https://doi.org/10.1016/j.apm.2009.11.021

4 Kanth, A.R., & Murali, M.K.P. (2018). A numerical technique for solving nonlinear singularly perturbed delay differential equations. *Mathematical Modelling and Analysis, 23*(1), 64–78. https://doi.org/10.3846/mma.2018.005

5 Kanth, A.R., & Murali, M.K.P. (2018). Numerical Method for a Class of Nonlinear Singularly Perturbed Delay Differential Equations Using Parametric Cubic Spline. *International Journal of Nonlinear Sciences and Numerical Simulation, 19*(3-4), 357–365. https://doi.org/10.1515/ijnsns-2017-0126

6 Lalu, M., & Phaneendra, K. (2022). A Numerical Approach for Singularly Perturbed Nonlinear Delay Differential Equations Using a Trigonometric Spline. *Computational and Mathematical Methods, 2022*, 8338661. https://doi.org/10.1155/2022/8338661

7 Chandru, M., Prabha, T., & Shanthi, V. (2015). A Hybrid Difference Scheme for a Second-Order Singularly Perturbed Reaction-Diffusion Problem with Non-smooth Data. *International Journal of Applied and Computational Mathematics, 1*, 87–100. https://doi.org/10.1007/s40819-014-0004-8

8 Sirisha, L., Phaneendra, K., & Reddy, Y.N. (2018). Mixed finite difference method for singularly perturbed differential difference equations with mixed shifts via domain decomposition. *Ain Shams Engineering Journal, 9*(4), 647–654. https://doi.org/10.1016/j.asej.2016.03.009

9 Subburayan, V., & Ramanujam, N. (2021). Uniformly Convergent Finite Difference Schemes for Singularly Perturbed Convection Diffusion Type Delay Differential Equations. *Differential Equations and Dynamical Systems, 29*, 139–155. https://doi.org/10.1007/s12591-018-00451-x

10 Woldaregay, M.M., & Duressa, G.F. (2020). Higher-Order Uniformly Convergent Numerical Scheme for Singularly Perturbed Differential Difference Equations with Mixed Small Shifts. *International Journal of Differential Equations, 2020*, 6661592. https://doi.org/10.1155/2020/6661592

11 Woldaregay, M.M., & Duressa, G.F. (2021). Robust mid-point upwind scheme for singularly perturbed delay differential equations. *Computational and Applied Mathematics, 40*, 178. https://doi.org/10.1007/s40314-021-01569-5

12 Ranjan, K.K., & Gowrisankar, S. (2022). Uniformly convergent NIPG method for singularly perturbed convection diffusion problem on Shishkin type meshes. *Applied Numerical Mathematics, 179*, 125–148. https://doi.org/10.1016/j.apnum.2022.04.015

13 Prathap, T., & Rao, R.N. (2023). A Higher Order Finite Difference Method for a Singularly Perturbed Boundary Value Problem with a Small Negative Shift. *International Journal of Applied and Computational Mathematics, 9*, 101. https://doi.org/10.1007/s40819-023-01578-4

14 Prathap, T., & Rao, R.N. (2024). Fitted mesh methods based on non-polynomial splines for singularly perturbed boundary value problems with mixed shifts. *AIMS Mathematics, 9*(10), 26403–26434. https://doi.org/10.3934/math.20241285

15 Chakravarthy, P.P., & Kumar, K. (2019). An adaptive mesh method for time dependent singularly perturbed differential-difference equations. *Nonlinear Engineering, 8*(1), 328–339. https://doi.org/10.1515/nleng-2018-0075

16 Kumar, D. (2018). An implicit scheme for singularly perturbed parabolic problem with retarded terms arising in computational neuroscience. *Numerical Methods for Partial Differential Equations, 34*, 1933–1952. https://doi.org/10.1002/num.22269

17 Ranjan, R., & Prasad, H.S. (2021). A novel approach for the numerical approximation to the solution of singularly perturbed differential-difference equations with small shifts. *Journal of Applied Mathematics and Computing, 65*, 403–427. https://doi.org/10.1007/s12190-020-01397-6

18 Rao, R.N., & Chakravarthy, P.P. (2019). Fitted numerical methods for singularly perturbed one-dimensional parabolic partial differential equations with small shifts arising in the modelling of neuronal variability. *Differential Equations and Dynamical Systems, 27*(1), 1–18. https://doi.org/10.1007/s12591-017-0363-9

19 Kiltu, G.G., Duressa, G.F., & Bullo, T.A. (2021). Computational method for singularly perturbed delay differential equations of the reaction-diffusion type with negative shift. *Journal of Ocean Engineering and Science, 6*(3), 285–291. https://doi.org/10.1016/j.joes.2021.02.001

20 Tefera, D.M., Tiruneh, A.A., & Derese, G.A. (2024). Fitted operator method for parabolic singularly perturbed convection-diffusion problems via polynomial cubic spline. *Journal of Applied Mathematics and Computing, 70*, 4655–4676. https://doi.org/10.1007/s12190-024-02153-w

21 Vivek, K., & Nageshwar Rao, R. (2024). Numerical algorithms based on splines for singularly perturbed parabolic partial differential equations with mixed shifts. *Boundary Value Problems,*

2024, 158. https://doi.org/10.1186/s13661-024-01971-y

22 Chakravarthy, P.P., Kumar, S.D., & Rao, R.N. (2017). Numerical solution of second order singularly perturbed delay differential equations via cubic spline in tension. *International Journal of Applied and Computational Mathematics, 3*, 1703–1717. https://doi.org/10.1007/s40819-016-0204-5

23 Hassen, Z.I., & Duressa, G.F. (2025). Parameter uniform finite difference formulation with oscillation free for solving singularly perturbed delay parabolic differential equation via exponential spline. *BMC Research Notes, 18*, 24. https://doi.org/10.1186/s13104-024-07005-1

24 Chawla, M.M. (1978). A Fourth-order Tridiagonal Finite Difference Method for General Nonlinear Two-point Boundary Value Problems with Mixed Boundary Conditions. *IMA Journal of Applied Mathematics, 21*(1), 83–93. https://doi.org/10.1093/imamat/21.1.83

25 Chawla, M.M. (1979). A Sixth-order Tridiagonal Finite Difference Method for General Nonlinear Two-point Boundary Value Problem. *IMA Journal of Applied Mathematics, 24*(1), 35–42. https://doi.org/10.1093/imamat/24.1.35

26 Bellman, R.E., & Kalaba, R.E. (1965). *Quasilinearization and Nonlinear Boundary Value Problems.* American Elsevier, New York.

27 Doolan, E.P., Miller, J.J.H., & Schilders, W.H.A. (1980). *Uniform Numerical Methods for Problems with Initial and Boundary Layers.* Boole Press, Dublin.

28 O'Malley, R.E. (1974). *Introduction to Singular Perturbations.* Academic Press, New York.

29 Varga, R.S. (1962). *Matrix Iterative Analysis.* Prentice-Hall Inc., Englewood Cliffs, New Jersey.

30 Young, D.M. (1971). *Iterative Solution of Large Linear Systems.* Academic Press, New York.

Author Information[*]

Theerthagiri Prathap — PhD Research Scholar, Department of Mathematics, School of Advanced Sciences, Vellore Institute of Technology, Vellore, 632 014, India; e-mail: *prathapkumar07@gmail.com*; https://orcid.org/0000-0002-7083-193X

Ragi Nageshwar Rao (*corresponding author*) — PhD in Mathematics, Associate Professor, Department of Mathematics, School of Advanced Sciences, Vellore Institute of Technology, Vellore, 632 014, India; e-mail: *nag.ragi@gmail.com*; https://orcid.org/0000-0003-4225-1927

[*]The author's name is presented in the order: First, Middle, and Last Names.